IEEE Access
Multidisciplinary | Rapid Review | Open Access Journal

Received February 5, 2019, accepted February 19, 2019, date of publication March 12, 2019, date of current version March 26, 2019.

Digital Object Identifier 10.1109/ACCESS.2019.2904171

Robust Learning Control for Robot Manipulators With Random Initial Errors and Iteration-Varying Reference Trajectories

QIUZHEN YAN[1], JIANPING CAI[2], YAN MA[1], AND YOUFANG YU[3]

[1]College of Information Engineering, Zhejiang University of Water Resources and Electric Power, Hangzhou 310018, China
[2]School of Electrical Engineering, Zhejiang University of Water Resources and Electric Power, Hangzhou 310018, China
[3]Applied Engineering College, Zhejiang Business College, Hangzhou 310053, China

Corresponding author: Qiuzhen Yan (zjhzyqz@gmail.com)

This work was part supported in part by the National Natural Science Foundation of China (NSFC) under Grant 61573322, in part by the Scientific Research Project of the Water Conservancy Department, Zhejiang, under Grant RC1858, and in part by the University Visiting Scholars Developing Project, Zhejiang, under Grant FX2017078.

ABSTRACT In this paper, we propose an error-tracking iterative learning control scheme to tackle the position tracking problem for robot manipulators with random initial errors and iteration-varying reference trajectories. Different from general usual ones, the control strategy in our work is to drive system errors perfectly track the desired error trajectories over the whole time interval as the iteration number increases, by which, the position trajectory and velocity trajectory can respectively track their reference trajectories during the predefined part operation interval. For fulfilling the control design, a new construction method of desired error trajectories is presented to remove the perfect initial resetting condition, which must be satisfied in most traditional iterative learning control algorithms. The uncertainties and disturbances in the robotic system dynamics are compensated by the robust approach and iterative learning approach, combinedly.

INDEX TERMS Iterative learning control, initial problem, robot manipulators.

I. INTRODUCTION

Iterative learning control (ILC) is suitable for designing control laws for repetitive control process over a finite time interval [1]–[8]. It pursues high-precision control performance through updating control input from cycle to cycle. In ILC designs, the dynamics of the system need not be known a priori. Nowadays, robot manipulators have been widely used to undertake repetitive tasks in assembly lines, rehabilitation processes, etc. In these situations, ILC is a proper technique to design control systems for obtaining good trajectory-tracking performances. Actually, numerous ILC algorithms for robotic applications have been reported right from the beginning of ILC research, i.e., the early 1980s [1], [9].

Adaptive ILC has attracted a lot of attentions since the beginning of this century [10]. Many achievements of adaptive ILC for robotic systems have witnessed the years of explorations and efforts. Most of these achievements focus on the position trajectory tracking of robotic systems [11]–[14].

The associate editor coordinating the review of this manuscript and approving it for publication was Xiaoli Luan.

In [11], three simple ILC schemes were proposed to deal with the trajectory tracking problem for rigid robot manipulators. In [12], a combined time-domain and iteration-domain learning strategy was developed for uncertain robot manipulators. In [13], an adaptive boundary ILC scheme was designed for a two−link rigid−flexible manipulator, aiming at achieving good trajectory tracking performance and eliminating deformation of flexible beam simultaneously. In [14], the iterative learning impedance control for rehabilitation robots was discussed. In these above-mentioned algorithms on ILC application to robot systems, the initial errors of robotic systems were assumed to be zero at each iteration cycle. Due to the limitation of practical resetting mechanism, it is yet difficult for actual robotic systems to implement such a zero-error initial resetting at the beginning of each iteration. Through continuous efforts, people have obtained a few promising results to solve the initial problem of ILC for normal nonlinear systems [15]–[20]. However, as far as the adaptive ILC design for robotic systems with random initial errors is concerned, the literature results have been still very few up to now. In the Remark 3 of [12], Chien *et al.* suggested that the time-varying boundary layer approach and the initial rectifying action may

be used to deal with the nonzero initial errors in ILC systems, but they did not present specific details. As reported in [21], initial rectifying action was used in the ILC design of upper limb rehabilitation robots. Besides, for the situations that reference trajectory is spatially closed, repetitive learning control is regarded as a remedy to remove zero-error initial resetting [22], [23], by adopting the final state of the previous iteration as the initial state of the current iteration. On the whole, in the adaptive ILC law design of robot manipulators, how to deal with random initial position/velocity errors is still an issue to be further studied.

On the other hand, in traditional ILC alogrithms, usually, the reference trajectory is iteration-invariant. However, in practical applications, the reference trajectories maybe change due to the variation of control objectives. Hence, it is of significance to investigate ILC algorithms suitable to the cases that reference trajectories varies in the iteration domain. The ILC research on tracking iteration-varying trajectories has arisen a lot of interests in the past two decades. In [24], Saab *et al.* investigated contraction-mapping ILC for systems with slowly iteration-varying reference trajectories. In [25], Xu *et al.* considered the adaptive ILC law design for cases that the target trajectories at the any two consecutive iterations are completely different. In [26], a novel adaptive iterative learning control approach is proposed to handle the non-uniform trajectory tracking problem for hybrid parametric nonlinear systems, with backstepping mechanism used to deduce the control law and learning law. Later, researchers have explored the ILC design for systems with iteration-varying trajectories and random initial condition [27]–[29]. As far as robotic ILC systems are concerned, in some cases, owing to the variation of control objectives or task specifications, the target trajectories will have to vary accordingly. Then, for robotic adaptive ILC algorithms designed only for iteration-invariant trajectory tracking, once the desired trajectory varies, even if the variation is very small, the robotic ILC systems will have to restart the learning process from the very beginning, and the previously learned information can not be used any more. In such cases, the robotic ILC schemes of tracking iteration-varying trajectories have higher efficiency. Since the robotic systems can learn consecutively from different tracking control tasks, therefore, there is no need to restart the learning process from the very beginning even if the target trajectory varies. In addition, for the robotic ILC systems which need simultaneously deal with distinct task trajectories in different cycles, one has no choice but to design proper ILC laws to achieve iteration-varying trajectory tracking. Up to now, few results consider the position-tracking issue of robot ILC systems with iteration-varying trajectories and random initial condition. Without perfect initial resetting, how to develop an effective ILC algorithm to meet the requirement of tracking iteration-varying trajectories, as well as to deal with the uncertainties in robot systems, is worthwhile to be researched.

This paper focuses on the trajectory-tracking problem for uncertain robot manipulators with random initial errors and iteration-varying trajectories. Compared to the existing results, the main contributions of this work lie in the following:

(1) By letting the system errors follow the constructed auxiliary signals over the whole interval, the position and velocity states of robotic systems can precisely track the target trajectories during the predefined part interval. The control strategy is different from traditional ILC ones. And the auxiliary signals, named as desired error trajectories in this paper, are constructed with the given construction method.

(2) Both random initial errors and iteration-varying reference trajectories are considered in the adaptive ILC design of uncertain robot systems.

(3) Adaptive learning technique and robust technique are applied together for compensating the parametric uncertainties and disturbances. Full saturation learning method is presented to estimate the unknown parameters and the upper bound of disturbances in uncertain robotic systems.

The remainder of this paper is organized as follows. In Section 2, an n degree-of-freedom manipulator is presented. In Section 3, the construction method of auxiliary signals is presented, and the robust learning controller is designed by using Lyapunov approach. In Section 4, through rigorous analysis, the uniform convergence of joint position and velocity tracking errors are shown. Also, the simulation results are illustrated in Section 5, followed by Section 6 which concludes this work.

II. PROBLEM FORMULATION

Let us consider an n degrees-of-freedom rigid manipulator with the dynamic equations is expressed by

$$M(q_k(t))\ddot{q}_k(t) + C(q_k(t), \dot{q}_k(t))\dot{q}_k(t) + G(q_k(t)) = \tau_k(t) + d_k(t), \quad (1)$$

where $k = 0, 1, 2, \cdots$ denotes the iteration index, $q_k = [q_{1,k}, q_{2,k}, \cdots, q_{n,k}]^T \in R^n$ is the vector of joint position at the kth iteration, $M(q_k(t)) \in R^{n\times n}$ is the symmetric positive definite manipulator inertia matrix, $C(q_k(t), \dot{q}_k(t))\dot{q}_k(t) \in R^n$ is the vector of centripetal and Coriolis torques, $G(q_k(t)) \in R^n$ is the vector of gravitational torques, $\tau_k(t) \in R^n$ is the control input vector containing the torques and forces to be applied at each joint, and $d_k(t) = [d_{1,k}, d_{2,k}, \cdots, d_{n,k}]^T \in R^n$ is the vector containing the unmodeled dynamics and other unknown external disturbances.

This paper studies the iterative learning control for the robot manipulators under the condition that $q_k(0) \neq q_d(0)$ and $\dot{q}_k(0) \neq \dot{q}_d(0)$. The control objective is to design a proper iterative learning control law $\tau_k(t), t \in [0, T]$ which guarantees the boundedness of $q_k(t), \dot{q}_k(t), \ddot{q}_k(t), \forall t \in [0, T]$, and make $q_k(t)$ follow the desired reference trajectory $q_d(t) = [q_{1,d}(t), q_{2,d}(t), \cdots, q_{n,d}(t)]^T$ for all $t \in [t_h, T]$ when k tends to infinity, with t_h a predetermined time point during $(0, T)$.

The properties of the dynamic model (1) are given in the following:

Property 1: The matrix $\dot{M}(q_k(t)) - 2C(q_k(t), \dot{q}_k(t))$ is skew symmetric, which means $x^T(\dot{M}(q_k)(t) - 2C(q_k(t), \dot{q}_k(t))x = 0, \forall x \in R^n$.

Property 2: There exists a vector $\theta \in R^m$, with components depending on manipulator parameters (masses, moments of inertia, etc.), such that

$$M(q_k(t))\dot{v} + C(q_k(t), \dot{q}_k(t))v + G(q_k(t)) = W(q_k, \dot{q}_k, v, \dot{v})\theta, \quad (2)$$

where $W(q_k, \dot{q}_k, v, \dot{v}) \in R^{n\times m}$ is the regression matrix, and $v \in R^n$ is a vector of smooth functions [30], [31].

In this paper, $M(q_k)(t)$, $C(q_k(t), \dot{q}_k(t))$ and $G(q_k(t))$ are respectively abbreviated as M_k, C_k and G_k for brevity, and arguments are sometimes omitted while no confusion occurs.

III. ADAPTIVE ILC DESIGN

A. CONSTRUCTION OF DESIRED ERROR TRAJECTORY

Let us define $\tilde{q}_k = [\tilde{q}_{1,k}, \tilde{q}_{2,k}, \cdots, \tilde{q}_{n,k}]^T = q_k - q_d, d\tilde{q}_k = [d\tilde{q}_{1,k}, d\tilde{q}_{2,k}, \cdots, d\tilde{q}_{n,k}]^T = \dot{q}_k - \dot{q}_d$. We call $\tilde{q}^*_k = [\tilde{q}^*_{1,k}, \tilde{q}^*_{2,k}, \cdots, \tilde{q}^*_{n,k}]^T$ and $d\tilde{q}^*_k = [d\tilde{q}^*_{1,k}, d\tilde{q}^*_{2,k}, \cdots, d\tilde{q}^*_{n,k}]^T$ the desired error trajectory of $\tilde{q}_k$ and $d\tilde{q}_k$ in this paper, which are constructed as following:

For $i = 1, 2, \cdots, n$, while $t_h \le t \le T$, let

$$\tilde{q}^*_{i,k}(t) = 0, \quad (3)$$

$$d\tilde{q}^*_{i,k}(t) = 0; \quad (4)$$

while $0 \le t < t_h$, let

$$\tilde{q}^*_{i,k}(t) = [\tilde{q}_{i,k}(0) + d\tilde{q}_{i,k}(0)\int_0^t \chi(\tau)d\tau]\chi(t) \quad (5)$$

$$d\tilde{q}^*_{i,k}(t) = \dot{\tilde{q}}^*_{i,k}(t) = \tilde{q}_{i,k}(0)\dot{\chi}(t) + d\tilde{q}_{i,k}(0)\chi^2(t) + d\tilde{q}_{i,k}(0)\int_0^t \chi(\tau)d\tau\dot{\chi}(t) \quad (6)$$

where

$$\chi(t) = \frac{10(t_h - t)^3}{t_h^3} - \frac{15(t_h - t)^4}{t_h^4} + \frac{6(t_h - t)^5}{t_h^5}.$$

From the above construction, we can see that if $\tilde{q}_{i,k}(t)$ may precisely track $\tilde{q}^*_{i,k}(t)$ for all $t \in [t_h, T]$, then we obtain the convergence from $q_{i,k}(t)$ to $q_{i,d}(t)$ during $t \in [t_h, T]$.

According to the above construction, we can see the following characteristics of desired error trajectories:

(a). $\tilde{q}^*_k(0) = \tilde{q}_k(0), d\tilde{q}^*_k(0) = d\tilde{q}_k(0), k = 0, 1, 2, \cdots$

(b). $\tilde{q}^*_k(t) = 0, d\tilde{q}^*_k(t) = 0, t \in [t_h, T]$

(c). $\ddot{\tilde{q}}^*_k(t)$ is continuous for $t \in (0, T)$.

Among them, the characteristic (a) is utilized to relax the zero-initial-error resetting condition. For more details, see Remark 2. According to the characteristic (b), if we can make $\tilde{q}^*_k(t)$ follow $\tilde{q}_k(t)$, and $d\tilde{q}_k(t)$ follow $d\tilde{q}^*_k(t)$ simultaneously for $t \in [t_h, T]$, then $q_k(t) = q_d(t), \dot{q}_k(t) = \dot{q}_d(t), \forall t \in [t_h, T]$ would be obtained. In addition, the characteristic (c) is helpful to guarantee the continuity of the control input to be designed.

In the next section, we will design an adaptive iterative learning controller which make $[\tilde{q}_{i,k}(t), d\tilde{q}_{i,k}(t)]^T$ perfectly track $[\tilde{q}^*_{i,k}(t), d\tilde{q}^*_{i,k}(t)]^T$ for all $t \in [0, T]$ as the iteration number k increases.

B. CONTROL DESIGN

To facilitate the subsequent control design and stability analysis, we define

$$\begin{aligned} z_k &= [z_{1,k}, z_{2,k}, \cdots, z_{n,k}]^T = \tilde{q}_k - \tilde{q}^*_k, \\ dz_k &= [dz_{1,k}, dz_{2,k}, \cdots, dz_{n,k}]^T = d\tilde{q}_k - d\tilde{q}^*_k, \\ s_k &= [s_{1,k}, s_{2,k}, \cdots, s_{n,k}]^T = dz_k + \alpha z_k \end{aligned} \quad (7)$$

and

$$s_{\phi k} = s_k - \phi \mathrm{sat}_1(\tfrac{s_k}{\phi}), \quad (8)$$

where both α and ϕ are positive constants. In this paper, the saturation function sat.$(\cdot)$ is defined as, for a scalar $\hat{a}$,

$$\mathrm{sat}_{\bar{a}}(\hat{a}) \triangleq \mathrm{sgn}(\hat{a})\min(|\hat{a}|, \bar{a}), \quad (9)$$

where $\bar{a}$ is the upper bound on the magnitude of $\hat{a}$, and $\mathrm{sgn}(\cdot)$ is the signum function. For a $m-$dimensional vector $\hat{a}$,

$$\mathrm{sat}_{\bar{a}}(\hat{a}) = [\mathrm{sat}_{\bar{a}}(\hat{a}_1), \mathrm{sat}_{\bar{a}}(\hat{a}_2), \cdots, \mathrm{sat}_{\bar{a}}(\hat{a}_m)]^T \quad (10)$$

According to the above definition,

$$\mathrm{sat}_1(\frac{s_k}{\phi}) \triangleq [\mathrm{sat}_1(\frac{s_{1,k}}{\phi}), \mathrm{sat}_1(\frac{s_{2,k}}{\phi}), \cdots, \mathrm{sat}_1(\frac{s_{n,k}}{\phi})]^T.$$

From (7), we have $s_k = \dot{q}_k - \dot{q}_d - \dot{\tilde{q}}^*_k + \alpha z_k$. Further, we can get

$$\dot{s}_k = \ddot{q}_k - \ddot{q}_{zk} \quad (11)$$

with $q_{zk} \triangleq q_d + \tilde{q}^*_k - \alpha\int_0^t z_k d\tau$.

To obtain the control law, we define a nonnegative function $V_k(t)$ as follows:

$$V_k = \frac{1}{2}s^T_{\phi k}M_k s_{\phi k} \quad (12)$$

After taking the time derivative of V_k, we have

$$\begin{aligned} \dot{V}_k &= s^T_{\phi k}(M_k\ddot{q}_k - M_k\ddot{q}_{zk}) + \frac{1}{2}s^T_{\phi k}\dot{M}_k s_{\phi k} \\ &= s^T_{\phi k}(\tau_k - C_k\dot{q}_k - G_k - M_k\ddot{q}_{zk}) + \frac{1}{2}s^T_{\phi k}\dot{M}_k s_{\phi k} + s^T_{\phi k}d_k \\ &= s^T_{\phi k}[\tau_k - C_k(s_{\phi k} + \dot{q}_{zk}) - G_k - M_k\ddot{q}_{zk}] \\ &\quad + \frac{1}{2}s^T_{\phi k}\dot{M}_k s_{\phi k} + s^T_{\phi k}d_k \end{aligned} \quad (13)$$

According to Property I and II, we can deduce that

$$-s^T_{\phi k}C_k s_{\phi k} + \frac{1}{2}s^T_{\phi k}\dot{M}_k s_{\phi k} = 0 \quad (14)$$

and

$$M_k\ddot{q}_{zk} + C_k\dot{q}_{zk} + G_k = W(q_k, \dot{q}_k, \dot{q}_{zk}, \ddot{q}_{zk})\theta, \quad (15)$$

respectively. Let W_k denote $W(q_k, \dot{q}_k, \dot{q}_{zk}, \ddot{q}_{zk})$ for brevity in the rest of this paper. Then, substituting (14) and (15) into (13), we get

$$\begin{aligned} \dot{V}_k &= s^T_{\phi k}(\tau_k - W_k\theta + d_k) \\ &\le s^T_{\phi k}(\tau_k - W_k\theta) + \sum_{j=1}^{n}(|s_{\phi k,j}|d_{j,\mathrm{m}}) \end{aligned} \quad (16)$$

where $d_{j,\mathrm{m}}$ is the upper bound of $d_{j,k}$. Based on (16), an iterative learning control law is designed as

$$\tau_k = -\mu s_{\phi k} + W_k\hat{\theta}_k - \hat{d}_k \mathrm{sat}_1(\frac{s_k}{\phi}), \tag{17}$$

$$\theta_k = \mathrm{sat}_{\bar{\theta}}(\hat{\theta}_k)$$
$$\hat{\theta}_k = \mathrm{sat}_{\bar{\theta}}(\hat{\theta}_{k-1}) - \gamma_1 W_k^T s_{\phi k} \tag{18}$$

and

$$\hat{d}_{j,k} = \mathrm{sat}_{\bar{d}}(\hat{d}^*_{j,k})$$
$$\hat{d}^*_{j,k} = \mathrm{sat}_{\bar{d}}(\hat{d}^*_{j,k-1}) + \gamma_2|s_{\phi k,j}|, \tag{19}$$

where $\mu > 0$ is a control gain, γ_1 and γ_2 are positive learning gains, $\hat{d}_k = \mathrm{diag}(\hat{d}_{1,k}, \hat{d}_{2,k}, \cdots, \hat{d}_{n,k})$ and $\hat{d}_{j,k}$ is used to estimate $d_{j,\mathrm{m}}$ for $j = 1, 2, \cdots, n$; $\hat{\theta}_{-1}(t) = 0, \hat{d}^*_{j,-1}(t) = 0, \forall t \in [0, T]$.

Remark 1: For $t \in [0, t_h)$,

$$\dot{\tilde{q}}^*_{i,k}(t) = \tilde{q}_{i,k}(0)\dot{\chi}(t) + d\tilde{q}_{i,k}(0)\chi^2(t) + d\tilde{q}_{i,k}(0)\int_0^t \chi(\tau)d\tau\dot{\chi}(t)$$

and

$$\ddot{\tilde{q}}^*_{i,k}(t) = \tilde{q}_{i,k}(0)\ddot{\chi}(t) + 2d\tilde{q}_{i,k}(0)\chi(t)\dot{\chi}(t) + d\tilde{q}_{i,k}(0)\int_0^t \chi(\tau)d\tau\ddot{\chi}(t) + d\tilde{q}_{i,k}(0)\chi(\tau)\dot{\chi}(t)$$

hold. For $t \in [t_h, T]$, $\dot{\tilde{q}}^*_{i,k}(t) = 0$, $\ddot{\tilde{q}}^*_{i,k}(t) = 0$. From the above equations and $\ddot{q}_{zk} = \ddot{q}_d + \ddot{\tilde{q}}^*_k - \alpha\dot{z}_k$, we can see that $\ddot{q}_k$ is not used in the design of control input τ_k.

IV. STABILITY ANALYSIS

Theorem 1: For the closed-loop system consisting of the plant (1), and the adaptive iterative learning control given by (17)-(19), all system variables are guaranteed to be bounded at each iteration, and the closed-loop system is stable in the sense that

$$|\tilde{q}_{j,k}(t)| \le \frac{\phi}{\alpha}, \quad |\dot{\tilde{q}}_{j,k}(t)| \le 2\phi, \ t \in [t_h, T], \ j = 1, 2, \cdots, n.$$

Proof: Part A. From (16) and (17), we obtain

$$\begin{aligned} V_k &\le \int_0^t s_{\phi k}^T(\tau_k - W_k\theta)d\tau + \int_0^t \sum_{j=1}^n |s_{\phi k,j}|d_{j,\mathrm{m}}d\tau \\ &= \int_0^t (-\mu s_{\phi k}^T s_{\phi k} + s_{\phi k}^T W_k\tilde{\theta}_k)d\tau \\ &\quad + \sum_{j=1}^n \int_0^t |s_{\phi k,j}|\tilde{d}_{j,k}d\tau \end{aligned} \tag{20}$$

where $\tilde{\theta}_k = \theta_k - \theta$, $\tilde{d}_{j,k} = d_{j,\mathrm{m}} - d_{j,k}$.

Let us define a Lyapunov functional at the kth iteration as

$$L_k = V_k + \frac{1}{2\gamma_1}\int_0^t \tilde{\theta}_k^T\tilde{\theta}_k d\tau + \frac{1}{2\gamma_2}\sum_{j=1}^n \int_0^t \tilde{d}^2_{j,k}d\tau, \tag{21}$$

in which γ_1 and γ_2 are positive constant gains. Then, we consider the difference of $L_k(t)$ with respect to iteration number. While $k > 0$, from (20) and (21), we obtain

$$\begin{aligned} &L_k - L_{k-1} \\ &\le V_k(0) - V_{k-1} + \sum_{j=1}^n \int_0^t |s_{\phi k,j}|\tilde{d}_{j,k}d\tau - \int_0^t \mu s_{\phi k}^T s_{\phi k}d\tau \\ &\quad + \int_0^t s_{\phi k}^T W_k\tilde{\theta}_k d\tau + \frac{1}{2\gamma_1}\int_0^t (\tilde{\theta}_k^T\tilde{\theta}_k - \tilde{\theta}_{k-1}^T\tilde{\theta}_{k-1})d\tau \\ &\quad + \frac{1}{2\gamma_2}\sum_{j=1}^n \int_0^t (\tilde{d}^2_{j,k} - \tilde{d}^2_{j,k-1})d\tau. \end{aligned} \tag{22}$$

Noting that

$$\begin{aligned} &\tilde{\theta}_k^T\tilde{\theta}_k - \tilde{\theta}_{k-1}^T\tilde{\theta}_{k-1} \\ &= -2(\theta - \theta_k)^T(\theta_k - \theta_{k-1}) - (\theta_k - \theta_{k-1})^T(\theta_k - \theta_{k-1}) \\ &\le 2\tilde{\theta}_k^T(\theta_k - \theta_{k-1}), \end{aligned} \tag{23}$$

we obtain the following expression:

$$\begin{aligned} &\frac{1}{2\gamma_1}(\tilde{\theta}_k^T\tilde{\theta}_k - \tilde{\theta}_{k-1}^T\tilde{\theta}_{k-1}) + s_{\phi k}^T W_k\tilde{\theta}_k \\ &\le \frac{1}{\gamma_1}[\tilde{\theta}_k^T(\theta_k - \theta_{k-1}) + \gamma_1 s_{\phi k}^T W_k\tilde{\theta}_k] \\ &= \frac{1}{\gamma_1}[\mathrm{sat}_{\bar{\theta}}(\hat{\theta}_k) - \theta]^T[\mathrm{sat}_{\bar{\theta}}(\hat{\theta}_k) - \hat{\theta}_k] \le 0, \end{aligned} \tag{24}$$

where (18) is used. According to (24), (22) can be rewritten as

$$\begin{aligned} L_k - L_{k-1} &\le V_k(0) - V_{k-1} + \sum_{j=1}^n \int_0^t |s_{\phi k,j}|\tilde{d}_{j,k}d\tau \\ &\quad + \frac{1}{2\gamma_2}\sum_{j=1}^n \int_0^t (\tilde{d}^2_{j,k} - \tilde{d}^2_{j,k-1})d\tau. \end{aligned} \tag{25}$$

Similar to (23) and (24), from (19), we have

$$\begin{aligned} &\frac{1}{2\gamma_2}(\tilde{d}^2_{j,k} - \tilde{d}^2_{j,k-1}) + |s_{\phi k,j}|\tilde{d}_{j,k} \\ &\le \frac{1}{\gamma_2}[\tilde{d}_{j,k}(\hat{d}_{j,k-1} - \hat{d}_{j,k}) + \gamma_2|s_{\phi k,j}|\tilde{d}_{j,k}] \\ &= \frac{1}{\gamma_2}[d_{j,m} - \mathrm{sat}_{\bar{d}}(\hat{d}^*_{j,k})][\hat{d}^*_{j,k} - \mathrm{sat}_{\bar{d}}(\hat{d}^*_{j,k})] \le 0. \end{aligned} \tag{26}$$

Substituting (26) into (25) yields

$$L_k - L_{k-1} \le V_k(0) - V_{k-1}. \tag{27}$$

According to the characteristic (a) of desired error trajectories, $V_k(0) = 0$. Then, it follows from (27) that

$$L_k \le L_0 - \frac{\lambda_m}{2}\sum_{j=0}^{k-1} s_{\phi j}^T s_{\phi j}, \tag{28}$$

where λ_m represents the smallest eigenvalue of matrix M_k.

Remark 2: Without the characteristic (a), $V_k(0) \neq 0$. One can not deduce the inequality (27) or similar inequalities. Then, the convergence of robotic ILC systems can be obtained.

Part B. Now, we will show that $L_0(t)$ is bounded for $t \in [0, T]$. While $k = 0$, taking the time-derivative of $L_0(t)$ leads to

$$\dot{L}_0 \leq -\mu s_{\phi 0}^T s_{\phi 0} + s_{\phi 0}^T W_0 \tilde{\theta}_0 + \sum_{j=1}^{n} (|s_{\phi 0,j}| d_{j,\mathrm{m}}) + \frac{1}{2\gamma_1} \tilde{\theta}_0^T \tilde{\theta}_0 + \frac{1}{2\gamma_2} \sum_{j=1}^{n} \tilde{d}_{j,0}^2. \quad (29)$$

From (18), we have

$$\begin{aligned} &\frac{1}{2\gamma_1} \tilde{\theta}_0^T \tilde{\theta}_0 + s_{\phi 0}^T W_0 \tilde{\theta}_0 \\ &= \frac{1}{2\gamma_1} (\theta_0 - \theta)^T (\theta_0 - \theta + 2\gamma_1 W_0 s_{\phi 0}) \\ &= \frac{1}{2\gamma_1} (\theta_0 - \theta)^T (\theta_0 - \theta - 2\hat{\theta}_0) \\ &= \frac{1}{2\gamma_1} (\theta_0 - \theta)^T (\theta_0 - \theta - 2\theta_0 + 2\theta_0 - 2\hat{\theta}_0) \\ &= \frac{1}{2\gamma_1} (\theta^T \theta - \theta_0^T \theta_0) + \frac{1}{\gamma_1} (\theta_0 - \theta)^T (\theta_0 - \hat{\theta}_0). \end{aligned} \quad (30)$$

Meanwhile,

$$\frac{1}{\gamma_1} (\theta_0 - \theta)^T (\theta_0 - \hat{\theta}_0) = \frac{1}{\gamma_1} (\mathrm{sat}(\hat{\theta}_0) - \theta)^T (\mathrm{sat}(\hat{\theta}_0) - \hat{\theta}_0), \leq 0 \quad (31)$$

Therefore, from the above three inequalities, we obtain

$$\dot{L}_0 \leq -\mu s_{\phi 0}^T s_{\phi 0} + \frac{1}{2\gamma_1} (\theta^T \theta - \theta_0^T \theta_0) + \sum_{j=1}^{n} (|s_{\phi 0,j}| d_{j,\mathrm{m}}) + \frac{1}{2\gamma_2} \sum_{j=1}^{n} \tilde{d}_{j,0}^2 \quad (32)$$

Similarly, from (19), we can conclude that

$$\sum_{j=1}^{n} (|s_{\phi k,j}| d_{j,\mathrm{m}}) + \frac{1}{2\gamma_2} \sum_{j=1}^{n} \tilde{d}_{j,0}^2 \leq \frac{1}{2\gamma_2} \sum_{j=1}^{n} (d_{j,\mathrm{m}}^2 - \hat{d}_{j,0}^2) \quad (33)$$

Combining (33) with (32), we assert

$$\dot{L}_0 \leq -\mu s_{\phi 0}^T s_{\phi 0} + \frac{1}{2\gamma_1} (\theta^T \theta - \theta_0^T \theta_0) + \frac{1}{2\gamma_2} \sum_{j=1}^{n} (d_{j,\mathrm{m}}^2 - \hat{d}_{j,0}^2)$$

According to the property of saturation function, it is easily to see that $L_0(t)$ is bounded for $t \in [0, T]$.

Part C. By utilizing the boundedness of $L_0(t)$, from (28), we can easily see

$$\lim_{k \to +\infty} s_{\phi k}^T s_{\phi k} = 0, \quad (34)$$

which implies $\lim_{k \to +\infty} |s_{\phi k,j}| = 0, j = 1, 2, \cdots, n$. This further deduce that

$$\lim_{k \to +\infty} |s_{j,k}| \leq \phi, \quad j = 1, 2, \cdots, n. \quad (35)$$

It follows from (35) that [32]

$$|\tilde{q}_{j,k}(t)| \leq \frac{\phi}{\alpha}, \quad |\dot{\tilde{q}}_{j,k}(t)| \leq 2\phi, \ t \in [t_h, T], \ j = 1, 2, \cdots, n. \quad (36)$$

For clarity, we give the simple deduction on the above conclusion as follows:

From (7), we can obtain,

$$\mathrm{e}^{\alpha t} \dot{z}_{j,k} + \alpha \mathrm{e}^{\alpha t} z_{j,k} = \mathrm{e}^{\alpha t} s_{j,k}. \quad (37)$$

Calculating the definite integrals on both sides of (37) from 0 to t yields

$$\mathrm{e}^{\alpha t} z_{j,k}(t) - \mathrm{e}^{\alpha t} z_{j,k}(0) = \int_0^t \mathrm{e}^{\alpha \tau} s_{j,k}(\tau) d\tau. \quad (38)$$

Note that $z_{j,k}(0) = 0$ holds. After performing some simple algebraic operations, we have

$$|z_{j,k}(t)| \leq \frac{\mathrm{e}^{-\alpha t}}{\alpha} (\mathrm{e}^{\alpha t} - 1) \phi \leq \frac{\phi}{\alpha}, \quad t \in [0, T] \quad (39)$$

which implies that

$$|\tilde{q}_{j,k}(t)| \leq \frac{\phi}{\alpha}, t \in [t_h, T], \quad j = 1, 2, \cdots, n. \quad (40)$$

In addition, according to (7), (35) and (39), we have

$$|\dot{z}_{j,k}(t)| \leq |s_{j,k}(t)| + \alpha |z_{j,k}(t)| \leq 2\phi, \quad t \in [0, T], \quad (41)$$

which implies that

$$|\dot{\tilde{q}}_{j,k}(t)| \leq 2\phi, \quad t \in [t_h, T], \ j = 1, 2, \cdots, n. \quad (42)$$

Combining (40) with (42), we obtain (36). ■

Through properly choosing α and ϕ, we can get high-precision tracking for the closed-loop robotic systems over $[t_h, T]$.

V. SIMULATION RESULTS

To verify the effectiveness of our proposed control scheme, a two degrees-of-freedom planar manipulator with revolute joints is considered as follows:

$$\begin{aligned} &\begin{bmatrix} M_{11}(q_{2,k}) & M_{12}(q_{2,k}) \\ M_{12}(q_{2,k}) & M_{22}(q_{2,k}) \end{bmatrix} \begin{bmatrix} \ddot{q}_{1,k} \\ \ddot{q}_{2,k} \end{bmatrix} \\ &+ \begin{bmatrix} -C_{12}(q_{2,k}) \dot{q}_{2,k} & -C_{12}(q_{2,k})(\dot{q}_{1,k} + \dot{q}_{2,k}) \\ C_{12}(q_{2,k}) \dot{q}_{1,k} & 0 \end{bmatrix} \begin{bmatrix} \dot{q}_{1,k} \\ \dot{q}_{2,k} \end{bmatrix} \\ &+ \begin{bmatrix} G_1(q_{1,k}, q_{2,k}) g \\ G_2(q_{1,k}, q_{2,k}) g \end{bmatrix} = \begin{bmatrix} \tau_{1,k} + d_{1,k} \\ \tau_{2,k} + d_{2,k} \end{bmatrix}, \end{aligned} \quad (43)$$

where

$$\begin{aligned} M_{11}(q_{2,k}) &= (m_1 + m_2) r_1^2 + m_2 r_2^2 + 2 m_1 m_2 \cos q_{2,k}, \\ M_{12}(q_{2,k}) &= m_2 r_2^2 + m_2 r_1 r_2 \cos(q_{2,k}), \\ M_{22}(q_{2,k}) &= m_2 r_2^2, \\ C_{12}(q_{2,k}) &= m_2 r_1 r_2 \sin(q_{2,k}), \\ G_1(q_{1,k}, q_{2,k}) &= (m_1 + m_2) r_1 \cos q_{2,k} \\ &\quad + m_2 r_2 \cos(q_{1,k} + q_{2,k}), \\ G_2(q_{1,k}, q_{2,k}) &= m_2 r_2 \cos(q_{1,k} + q_{2,k}), \end{aligned} \quad (44)$$

and parametric uncertainties are $m_1 = 0.5$kg, $m_2 = 0.5$kg. The robot parameters are given by $r_1 = 1$m, $r_2 = 0.8$m, $g = 9.8\mathrm{m/s}^2$. The disturbances are assumed to be

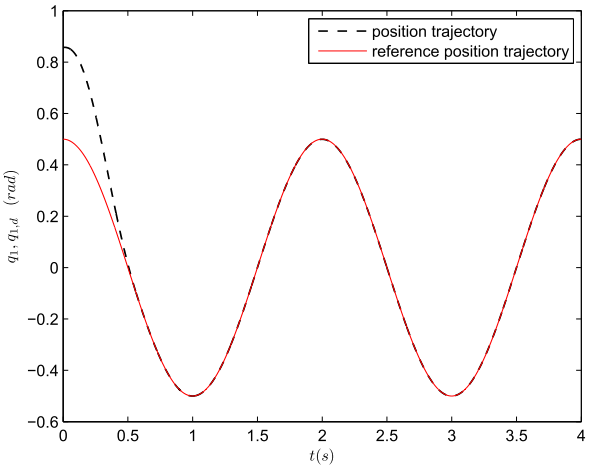

FIGURE 1. Actual and reference position trajectory of joint 1 ($k = 20$, error tracking ILC).

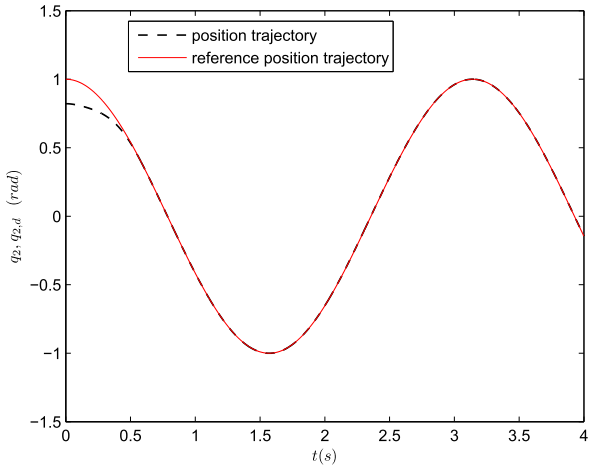

FIGURE 3. Actual and reference position trajectory of joint 2 ($k = 20$, error tracking ILC).

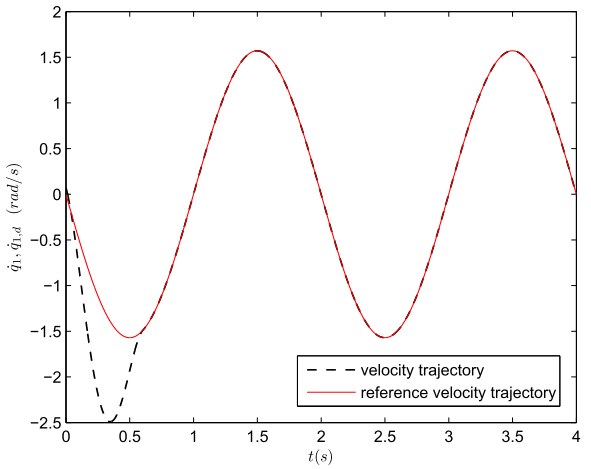

FIGURE 2. Actual and reference velocity trajectory of joint 1 ($k = 20$, error tracking ILC).

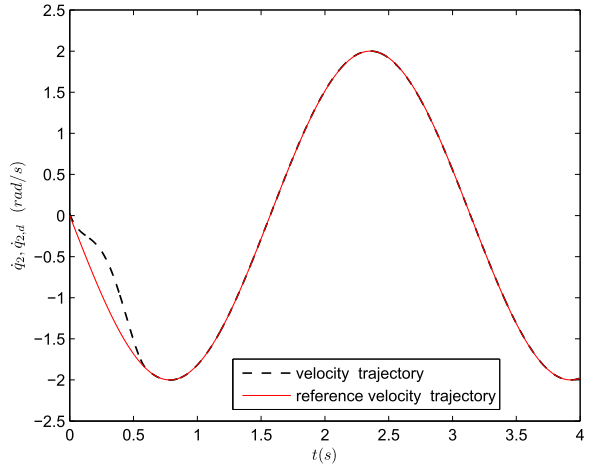

FIGURE 4. Actual and reference velocity trajectory of joint 2 ($k = 20$, error tracking ILC).

$d_{1,k} = 0.5\text{rand1}(k)\cos(t)$, $d_{2,k} = 0.5\text{rand2}(k)\sin(t)$. The initial states of robot manipulator are as follows:

$$\begin{cases} q_{1,k}(0) = 0.8 + 0.1\text{rand3}(k), \\ dq_{1,k}(0) = 0.05 + 0.05\text{rand4}(k), \\ q_{2,k}(0) = 0.82 + 0.1\text{rand5}(k), \\ dq_{2,k}(0) = 0.05\text{rand6}(k), \end{cases} \tag{45}$$

where, $\text{rand1}(\cdot) - \text{rand6}(\cdot)$ are random functions taking their values between 0 and 1. The reference position trajectories of q_1 and q_2 are respectively chosen as

$$q_{1,d}(t) = \begin{cases} 0.5\cos(\pi t) & k = 0, 2, 4, 6, \cdots \\ 1.2 + \dfrac{t^2}{10} - \dfrac{2t}{5} & k = 1, 3, 5, 7, \cdots \end{cases} \tag{46}$$

and

$$q_{2,d}(t) = \begin{cases} \cos(2t) & k = 0, 2, 4, 6, \cdots \\ 1 + \dfrac{2t}{5} - \dfrac{t^2}{10} & k = 1, 3, 5, 7, \cdots, \end{cases} \tag{47}$$

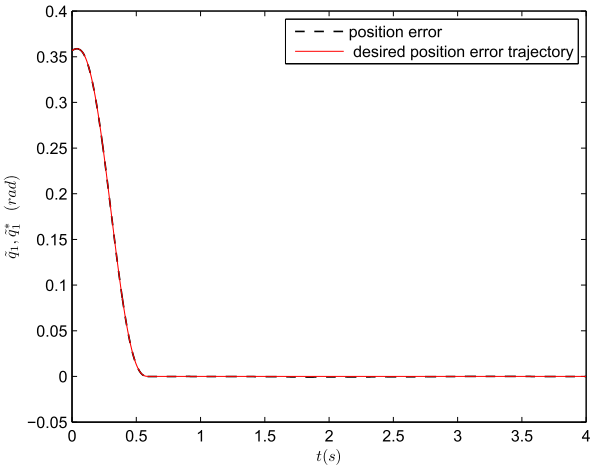

FIGURE 5. Position error and desired position error trajectory of joint 1 ($k = 20$, error tracking ILC).

with $\dot{q}_{1,d}(t)$ and $\dot{q}_{2,d}(t)$ being the corresponding reference velocity trajectories. Corresponding to (15), we take the

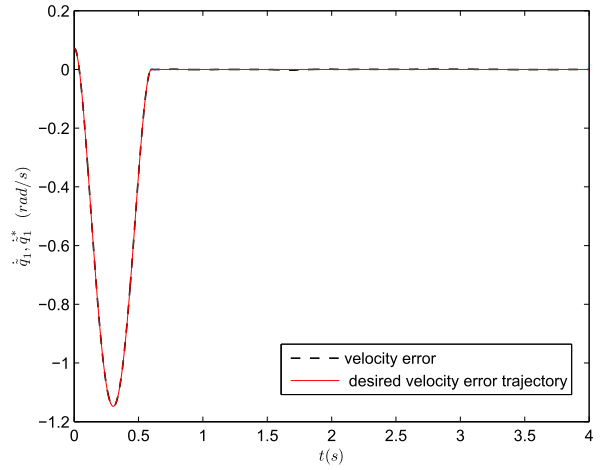

FIGURE 6. Velocity error and desired velocity error trajectory of joint 1 ($k = 20$, error tracking ILC).

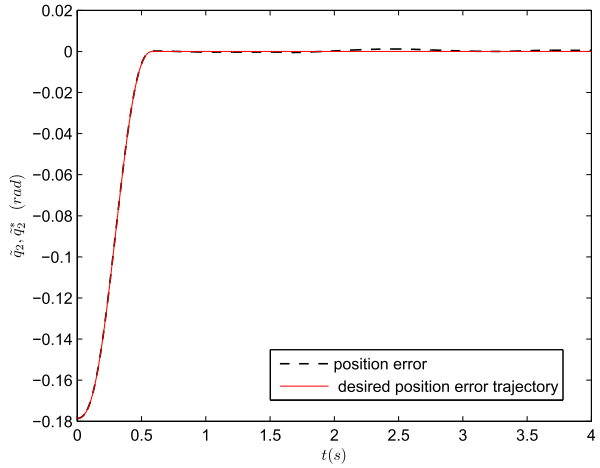

FIGURE 7. Position error and desired position error trajectory of joint 2 ($k = 20$, error tracking ILC).

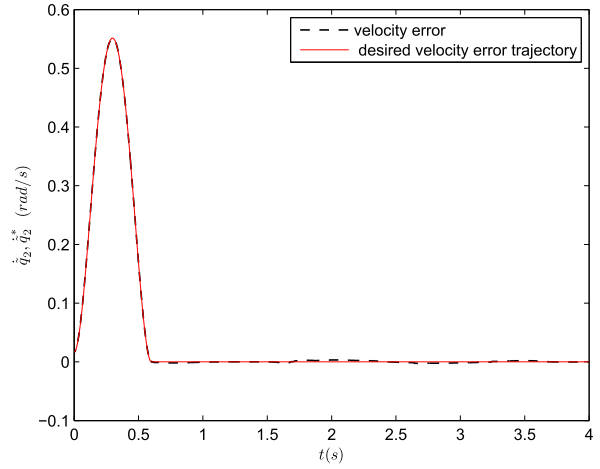

FIGURE 8. Velocity error and desired velocity error trajectory of joint 2 ($k = 20$, error tracking ILC).

following parameterization:

$$\begin{bmatrix} M_{11}(q_{2,k}) & M_{12}(q_{2,k}) \\ M_{12}(q_{2,k}) & M_{22}(q_{2,k}) \end{bmatrix} \begin{bmatrix} \ddot{q}_{zk,1} \\ \ddot{q}_{zk,2} \end{bmatrix}$$

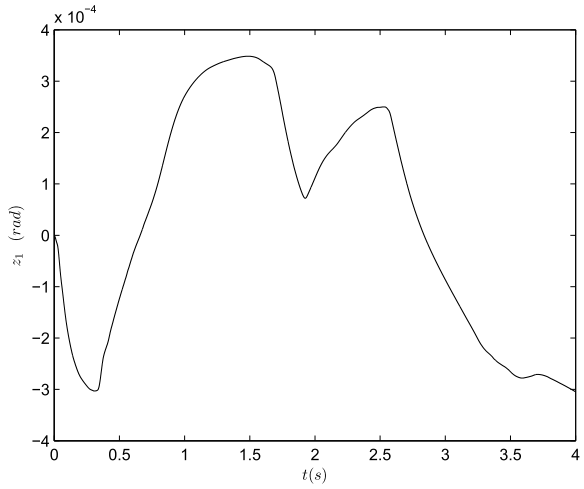

FIGURE 9. Difference between $\tilde{q}_1$ and $\tilde{q}_1^*$ ($k = 20$, error tracking ILC).

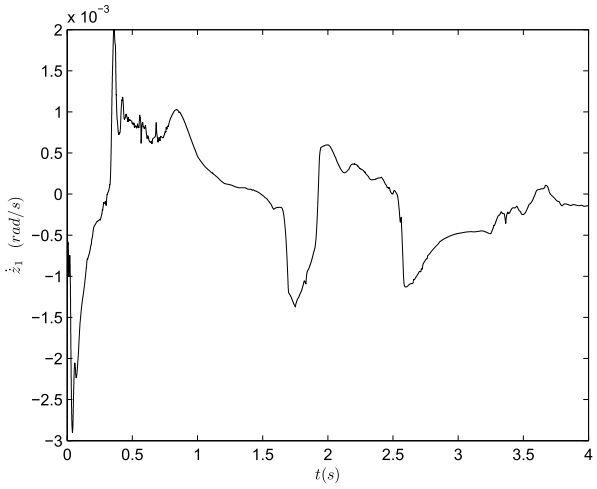

FIGURE 10. Difference between $\dot{\tilde{q}}_1$ and $\dot{\tilde{q}}_1^*$($k = 20$, error tracking ILC).

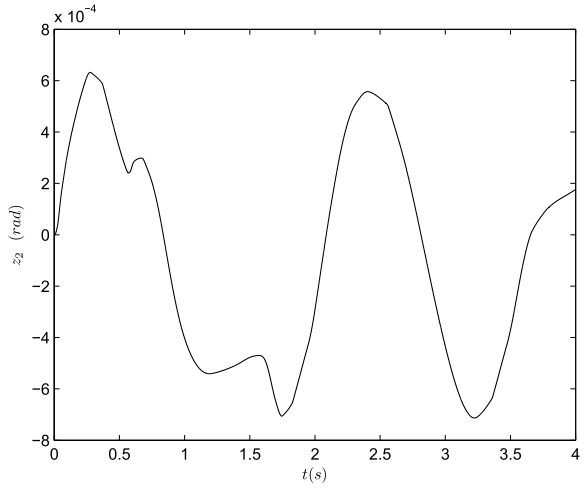

FIGURE 11. Difference between $\tilde{q}_2$ and $\tilde{q}_2^*$ ($k = 20$, error tracking ILC).

$$+ \begin{bmatrix} -C_{12}(q_{2,k})\dot{q}_{2,k} & -C_{12}(q_{2,k})(\dot{q}_{1,k} + \dot{q}_{2,k}) \\ C_{12}(q_{2,k})\dot{q}_{1,k} & 0 \end{bmatrix} \begin{bmatrix} \dot{q}_{zk,1} \\ \dot{q}_{zk,2} \end{bmatrix}$$

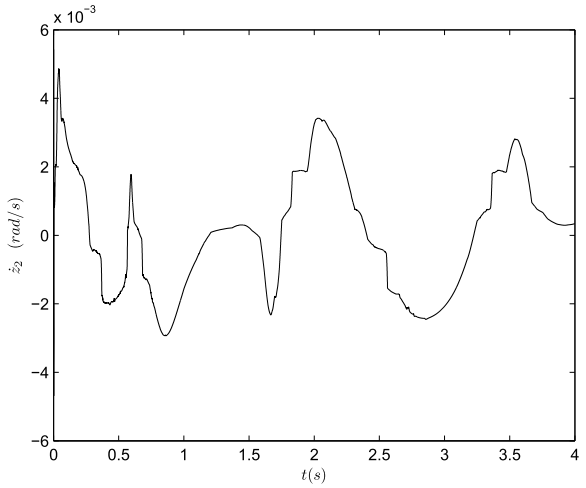

FIGURE 12. Difference between $\dot{\tilde{q}}_2$ and $\dot{\tilde{q}}_2^*$ ($k = 20$, error tracking ILC).

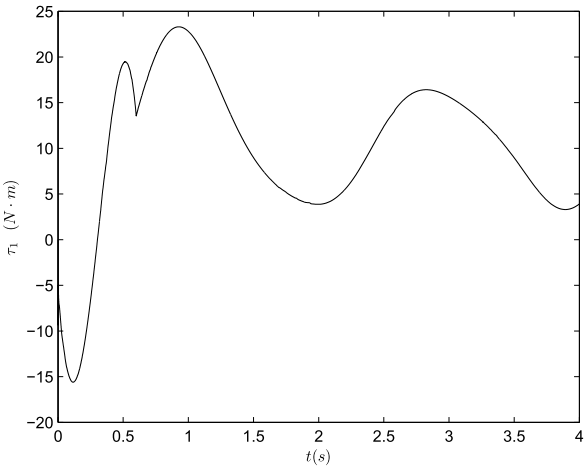

FIGURE 13. Control input of joint 1 ($k = 20$, error tracking ILC).

$$+\begin{bmatrix} G_1(q_{1,k}, q_{2,k})g \\ G_2(q_{1,k}, q_{2,k})g \end{bmatrix} = \begin{bmatrix} w_{z1} & w_{z2} & w_{z3} \\ w_{z4} & w_{z5} & w_{z6} \end{bmatrix} \begin{bmatrix} \theta_1 \\ \theta_2 \\ \theta_3 \end{bmatrix}$$

where

$$\begin{aligned}
w_{z1} &= \ddot{q}_{zk,1} + g/r_1 \cos q_{2,k}, \\
w_{z2} &= \ddot{q}_{zk,1} + \ddot{q}_{zk,2}, \\
w_{z3} &= 2\ddot{q}_{zk,1} \cos q_{2,k} + \ddot{q}_{zk,2} \cos q_{2,k} - \dot{q}_{2,k}\dot{q}_{zk,1} \sin q_{2,k} \\
&\quad - (\dot{q}_{1,k} + \dot{q}_{2,k})\dot{q}_{zk,2} \sin q_{2,k} + g/r_1 \cos(q_{1,k} + q_{2,k}), \\
w_{z4} &= 0, \\
w_{z5} &= w_{z2}, \\
w_{z6} &= \dot{q}_{1,k}\dot{q}_{zk,1} \sin q_{2,k} \\
&\quad + \ddot{q}_{zk,1} \cos q_{2,k} + g/r_1 \cos(q_{1,k} + q_{2,k}) \\
\theta_1 &= (m_1 + m_2)r_1^2, \\
\theta_2 &= m_2 r_2^2, \\
\theta_3 &= m_2 r_1 r_2. \qquad (48)
\end{aligned}$$

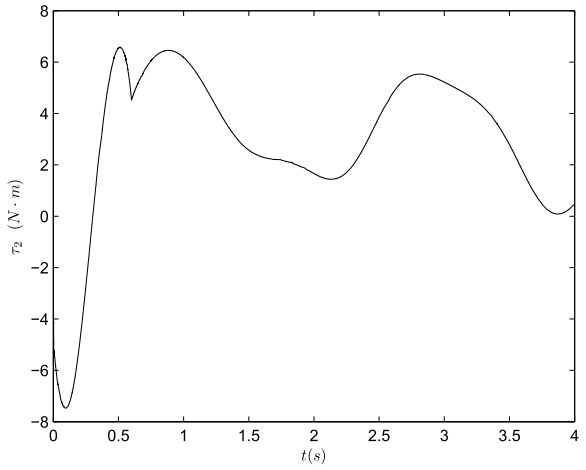

FIGURE 14. Control input of joint 2 ($k = 20$, error tracking ILC).

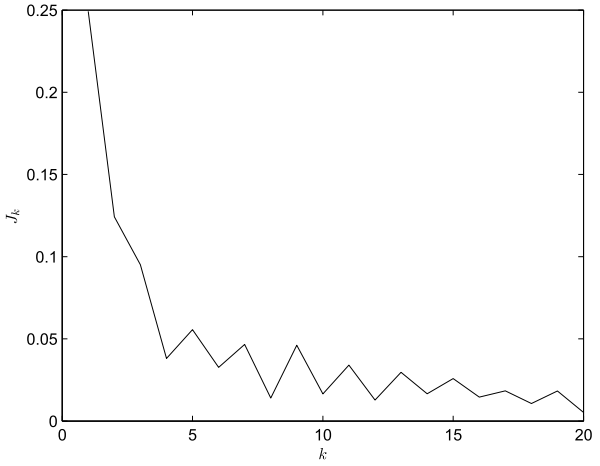

FIGURE 15. Convergence learning history of $\|s_{\phi k}\|$ (error tracking ILC).

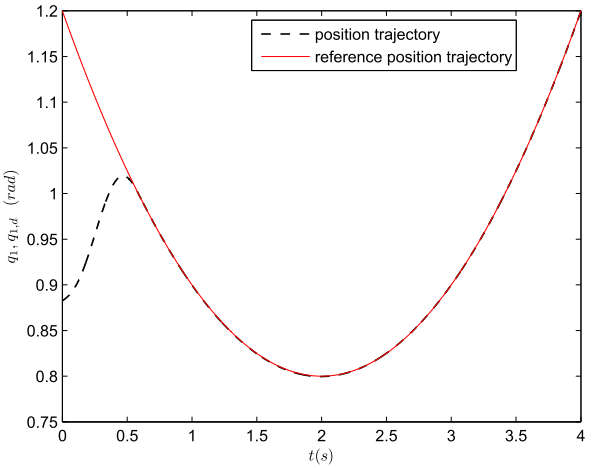

FIGURE 16. Actual and reference position trajectory of joint 1 ($k = 19$, error tracking ILC).

Applying the control law (17)−(19), with $\mu = 5$, $\gamma_1 = 1.2$, $\gamma_2 = 0.6, \phi = 0.0005$, $\bar{\theta} = 20, \bar{d} = 5$,

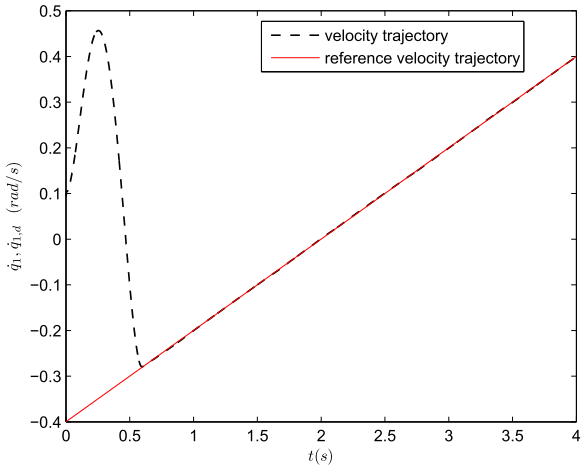

FIGURE 17. Actual and reference velocity trajectory of joint 1 ($k = 19$, error tracking ILC).

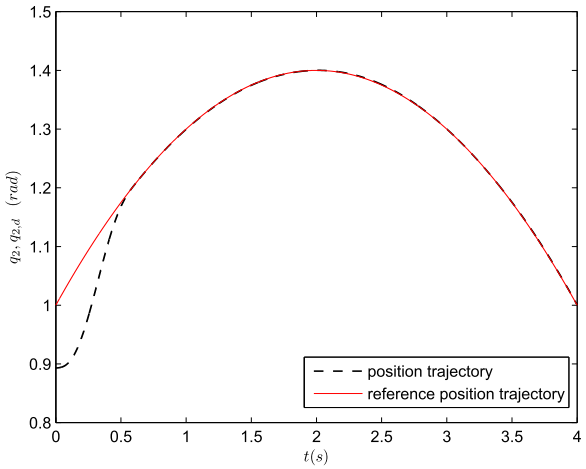

FIGURE 18. Actual and reference position trajectory of joint 2 ($k = 19$, error tracking ILC).

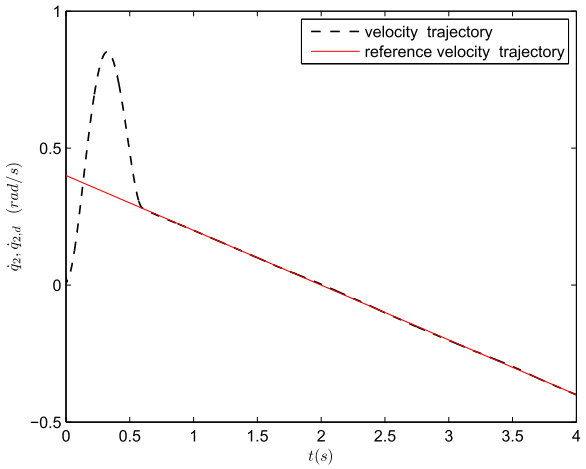

FIGURE 19. Actual and reference velocity trajectory of joint 2 ($k = 19$, error tracking ILC).

$T = 4s$ and $t_h = 0.6s$, we obtain the results shown in Figs. 1−29 after 20 cycles. The position/velocity trajectory profiles of joint 1 and joint 2 at the 20th cycle are shown

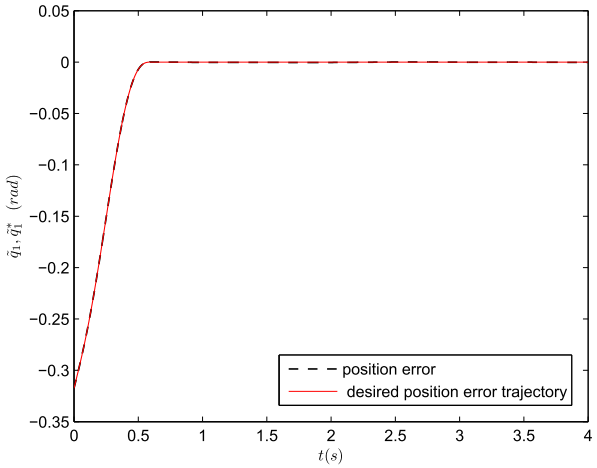

FIGURE 20. Position error and desired position error trajectory of joint 1 ($k = 19$, error tracking ILC).

in Figs. 1–4, respectively. We can see that the position/velocity trajectories accurately track their reference trajectories for $t \in [t_h, T]$. Figs.5−8 give the profiles of position/velocity errors and the desired error trajectories at the 20th iteration, followed by Figs. 9−12 which show the difference between the errors and the desired error trajectories. From Fig. 5−12, we can see that the error trajectories follow the desired error trajectories, respectively. Figs.13−14 plot the control inputs of joint 1 and 2, respectively. From Fig.15, we can see $s_{\phi k}$ converges to zero as the iteration number increase, where $J_k \triangleq \max_{t\in[0,T]} \|s_{\phi k}(t)\|$.

The simulation results at the 19th cycle are shown in Figs. 16−29, which are similar to Figs. 1−14. Combining Figs. 1−4 and Figs. 16−19, we can see that the position/velocity trajectories can accurately track the reference trajectories for $t \in [t_h, T]$, even if the reference trajectories are iteration-varying.

For comparison, we perform the simulation for the initial-rectifying adaptive ILC algorithm of robotic manipulators. Due to the existence of non-zero initial errors, the reference trajectory $q_d = [q_{1,d}, q_{2,d}]^T$ should be rectified, and the rectified reference position trajectories $q_{i,k,r}(t), i = 1, 2$ should meet the following four requirement:

1. $q_{i,k,r}(0) = q_{i,k}(0)$;
2. $\dot{q}_{1,k,r}(0) = \dot{q}_{i,k}(0)$;
3. $q_{i,k,r}(t) = q_{i,d}(t), \dot{q}_{i,k,r}(t) = \dot{q}_{i,d}(t)$ and $\ddot{q}_{i,k,r}(t) = \ddot{q}_{i,d}(t)$ hold for $t \in [t_h, T]$;
4. $q_{i,k,r}(t), \dot{q}_{i,k,r}(t)$ and $\ddot{q}_{i,k,r}(t)$ are continuous over the entire interval, in particular, including $t = t_h$.

According to the above requirement, a practicable construction strategy is [33], [34]

$$q_{i,k,r}(t) = \xi_i \cdot q^r_{i,k}(t) + (1 - \xi_i) \cdot x_{i,d}(t), \tag{49}$$

with

$$\xi_i = \begin{cases} 1 & \text{for } t \in [0, t_h), \\ 0 & \text{for } t \in [t_h, T], \end{cases} \tag{50}$$

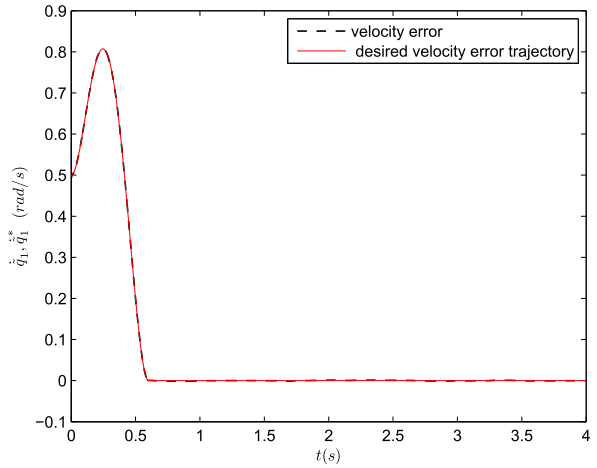

FIGURE 21. Velocity error and desired velocity error trajectory of joint 1 ($k = 19$, error tracking ILC).

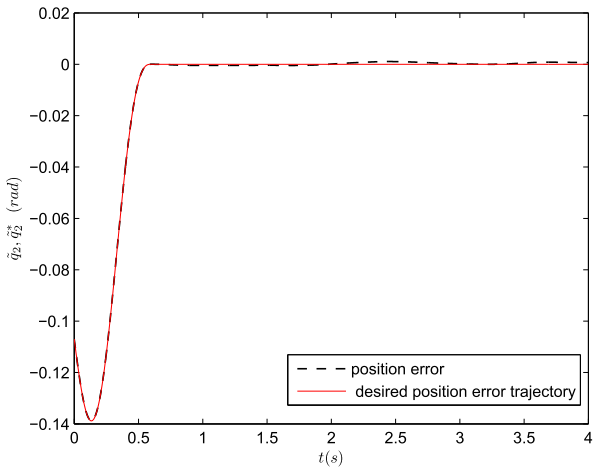

FIGURE 22. Position error and desired position error trajectory of joint 2 ($k = 19$, error tracking ILC).

and $q_{i,k}^r(t)$ is a smooth-connection curve to be formed. Then, let

$$q_{i,k}^r(t) = A_{i,5}t^5 + A_{i,4}t^4 + A_{i,3}t^3 + A_{i,2}t^2 + A_{i,1}t + A_{i,0}, \tag{51}$$

where $A_{i,0} = q_{i,k}(0), A_{i,1} = \dot{q}_{i,k}(0), A_{i,2} = 0,$

$$\begin{cases} A_{i,3} = \dfrac{10}{t_h^3}\varrho_1 - \dfrac{4}{t_h^2}\varrho_2 + \dfrac{1}{2t_h}\varrho_3, \\ A_{i,4} = -\dfrac{15}{t_h^4}\varrho_1 + \dfrac{7}{t_h^3}\varrho_2 - \dfrac{1}{t_h^2}\varrho_3, \\ A_{i,5} = \dfrac{6}{t_h^5}\varrho_1 - \dfrac{3}{t_h^4}\varrho_2 + \dfrac{1}{2t_h^3}\varrho_3, \end{cases} \tag{52}$$

with $\varrho_1 = q_{i,d}(t_h) - \dot{q}_{i,k}(0)t_h - q_{i,k}(0)$, $\varrho_2 = \dot{q}_{i,d}(t_h) - \dot{q}_{i,k}(0)$, $\varrho_3 = \ddot{q}_{i,d}(t_h)$.

After defining $q_{k,r} = [q_{1,k,r}, q_{2,k,r}]^T$, $s_{\varpi k} = (\dot{q}_k - \dot{q}_{k,r}) + \alpha(q_k - q_{k,r})$, $s_{vk} = s_{\varpi k} - v\mathrm{sat}_1(\frac{s_{\varpi k}}{v})$, we apply the following

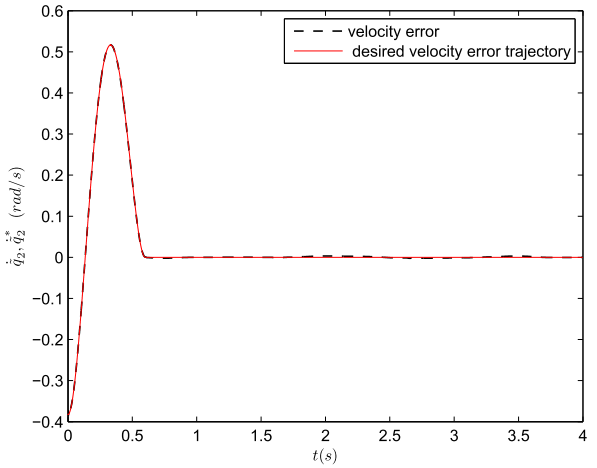

FIGURE 23. Velocity error and desired velocity error trajectory of joint 2 ($k = 19$, error tracking ILC).

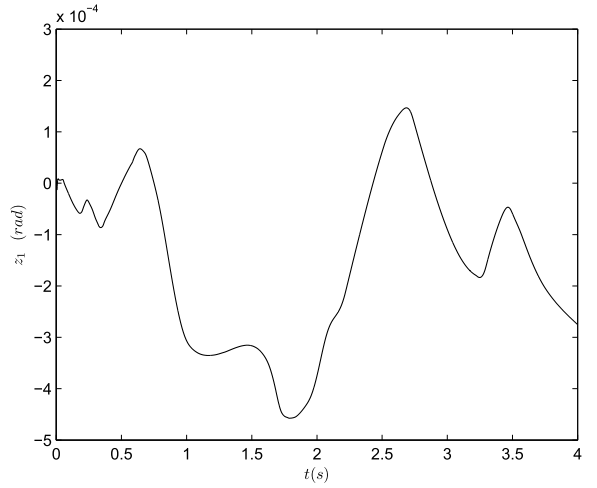

FIGURE 24. Difference between $\tilde{q}_1$ and $\tilde{q}_1^*$ ($k = 19$, error tracking ILC).

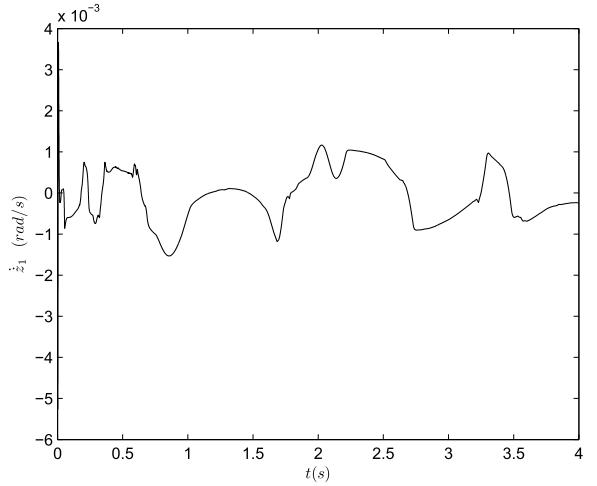

FIGURE 25. Difference between $\dot{\tilde{q}}_1$ and $\dot{\tilde{q}}_1^*$ ($k = 19$, error tracking ILC).

adaptive ILC control law and learning laws:

$$\tau_k = -\mu s_{vk} + W(q_k, \dot{q}_k, \dot{q}_{k,r}, \ddot{q}_{k,r})\hat{\theta}_k - \hat{d}_k\mathrm{sat}_1(\frac{s_{\varpi k}}{v}), \tag{53}$$

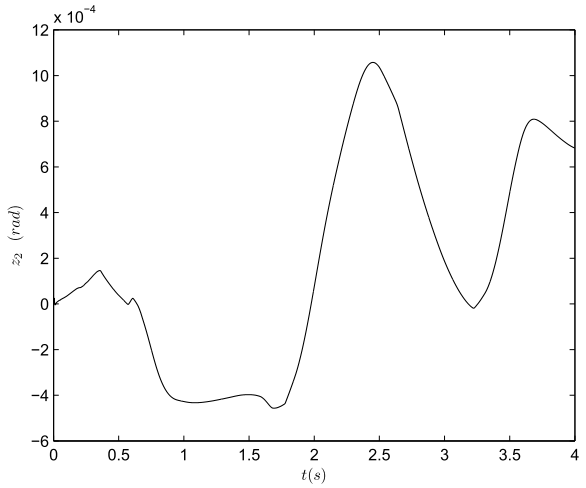

FIGURE 26. Difference between $\tilde{q}_2$ and $\tilde{q}_2^*$ ($k = 19$, error tracking ILC).

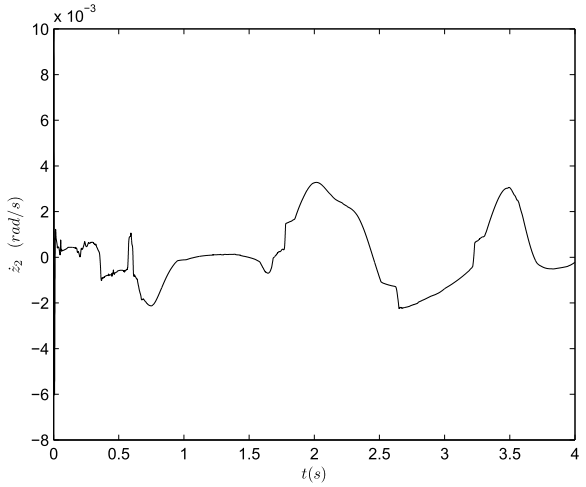

FIGURE 27. Difference between $\dot{\tilde{q}}_2$ and $\dot{\tilde{q}}_2^*$ ($k = 19$, error tracking ILC).

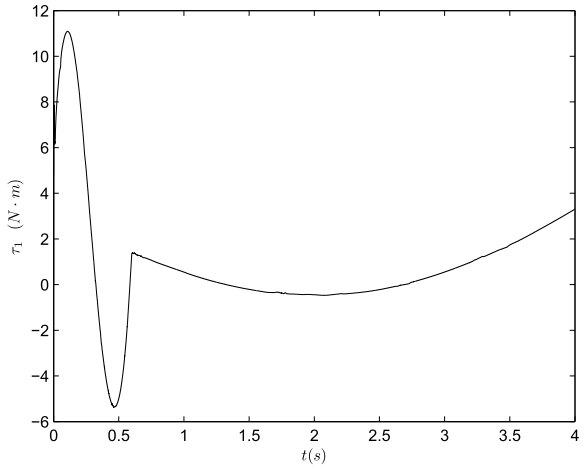

FIGURE 28. Control input of joint 1 ($k = 19$, error tracking ILC).

$$\begin{aligned}\theta_k &= \mathrm{sat}_{\bar{\theta}}(\hat{\theta}_k),\\ \hat{\theta}_k &= \mathrm{sat}_{\bar{\theta}}(\hat{\theta}_{k-1}) - \gamma_1 W(q_k, \dot{q}_k, \dot{q}_{k,r}, \ddot{q}_{k,r}) s_{vk}, \end{aligned} \tag{54}$$

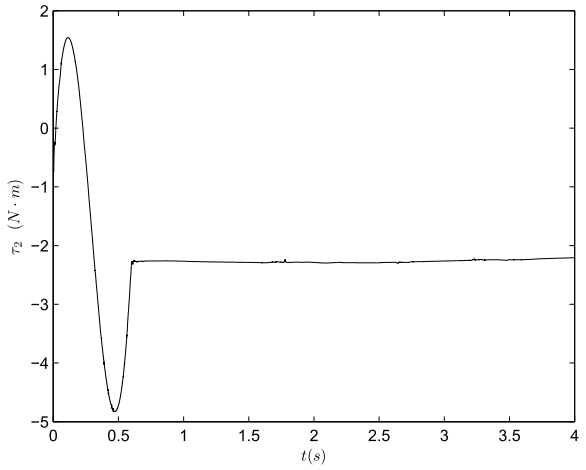

FIGURE 29. Control input of joint 2 ($k = 19$, error tracking ILC).

and

$$\begin{aligned}\hat{d}_{j,k} &= \mathrm{sat}_{\bar{d}}(\hat{d}^*_{j,k}),\\ \hat{d}^*_{j,k} &= \mathrm{sat}_{\bar{d}}(\hat{d}^*_{k,-1}) + \gamma_2 |s_{vk,j}|, \end{aligned} \tag{55}$$

where $\hat{\theta}_{-1} = 0$, $\hat{d}^*_{j,-1} = 0$,

$$W(q_k, \dot{q}_k, \dot{q}_{k,r}, \ddot{q}_{k,r}) = \begin{bmatrix} w_{r1} & w_{r2} & w_{r3} \\ w_{r4} & w_{r5} & w_{r6} \end{bmatrix}, \tag{56}$$

with

$$\begin{aligned}
w_{r1} &= \ddot{q}_{1,k,r} + g/r_1 \cos q_{2,k},\\
w_{r2} &= \ddot{q}_{1,k,r} + \ddot{q}_{2,k,r},\\
w_{r3} &= 2\ddot{q}_{1,k,r} \cos q_{2,k} + \ddot{q}_{2,k,r} \cos q_{2,k} - \dot{q}_{2,k}\dot{q}_{1,k,r} \sin q_{2,k}\\
&\quad - (\dot{q}_{1,k} + \dot{q}_{2,k})\dot{q}_{2,k,r} \sin q_{2,k} + g/r_1 \cos(q_{1,k} + q_{2,k}),\\
w_{r4} &= 0,\\
w_{r5} &= w_{d2},\\
w_{r6} &= \dot{q}_{1,k}\dot{q}_{1,k,r} \sin q_{2,k} + \ddot{q}_{1,k,r} \cos q_{2,k} + g/r_1 \cos(q_{1,k}\\
&\quad + q_{2,k}).
\end{aligned}$$

The control parameter are set: $v = 0.0005$, others are the same as the ones in the previous simulation. The initial state is chosen as (45). After 20 cycles, the simulation results are presented in Figs. 30–46. Among these figures, Figs. 30–33 show the position/velocity trajectory profiles at the 20th cycle, while Figs. 39–42 show the position/velocity trajectory profiles at the 19th cycle. The difference between position/velocity trajectories and the corresponding rectified reference trajectories at the 20th cycle are presented in Figs. 34–37, and the ones at the 19 cycle are presented in Figs. 43–46. From these above-mentioned figures, we can see that $q_k(t)$ and $\dot{q}_k(t)$ can accurately track $q_d(t)$ and $\dot{q}_d(t)$ for $t \in [t_h, T]$, respectively. The learning convergence history during 20 cycles is shown in Fig. 38, where $J_{vk} \triangleq \max_{t\in[0,T]} \|s_{vk}(t)\|$. We can see that initial rectifying ILC is also effective to solve the trajectory tracking problem for robotic systems.

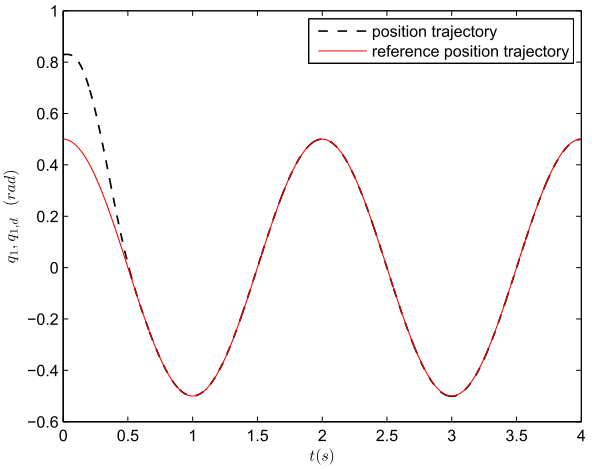

FIGURE 30. Actual and reference position trajectory of joint 1 ($k = 20$, initial rectifying ILC).

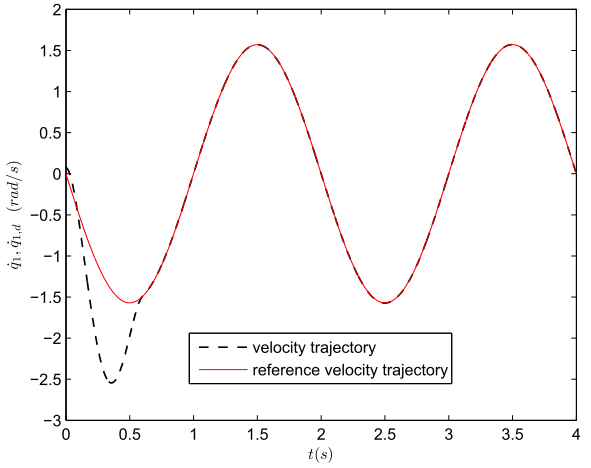

FIGURE 31. Actual and reference velocity trajectory of joint 1 ($k = 20$, initial rectifying ILC).

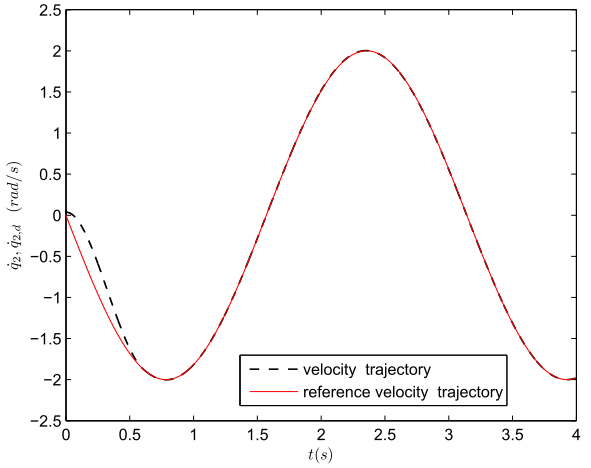

FIGURE 32. Actual and reference position trajectory of joint 2 ($k = 20$, initial rectifying ILC).

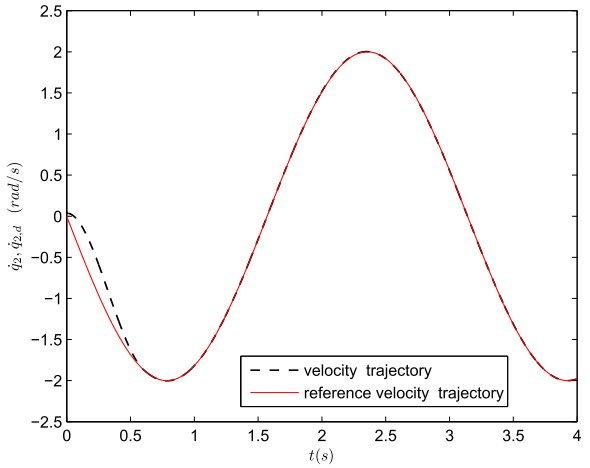

FIGURE 33. Actual and reference velocity trajectory of joint 2 ($k = 20$, initial rectifying ILC).

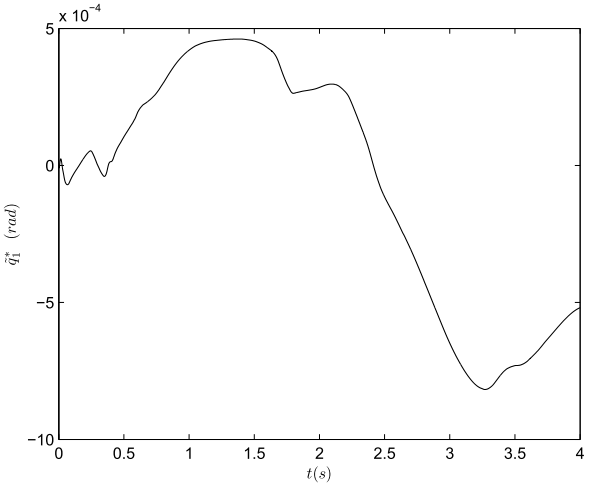

FIGURE 34. Difference between q_1 and q_1^* ($k = 20$, initial rectifying ILC).

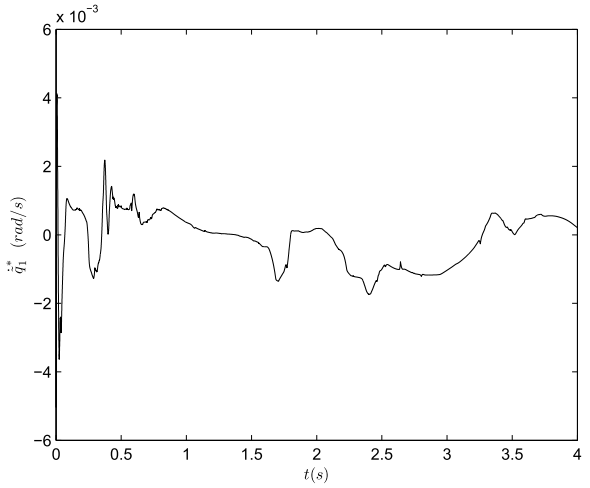

FIGURE 35. Difference between $\dot{q}_2$ and $\dot{q}_2^*$ ($k = 20$, initial rectifying ILC).

Comparing Figs. 8–12 with Figs. 34–37, we can see that the error tracking ILC and initial rectifying ILC have almost same tracking accuracy at the 20th cycle. Comparing Figs. 24–27 with Figs. 43–46, we can see that, at the 19th

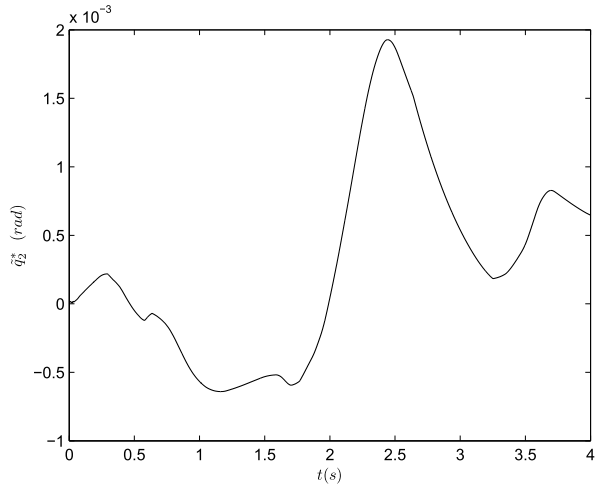

FIGURE 36. Difference between q_2 and q_2^* ($k = 20$, initial rectifying ILC).

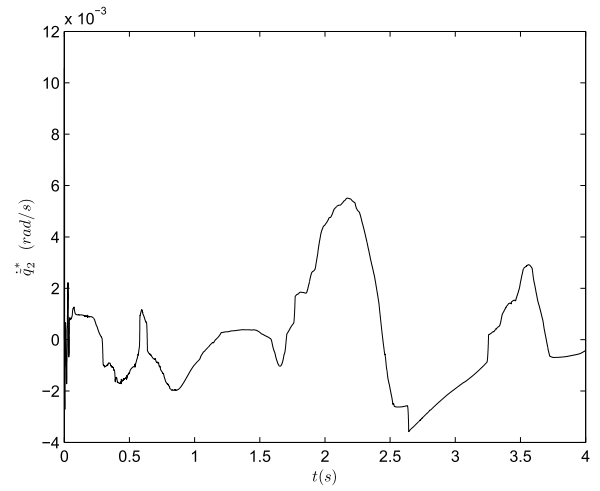

FIGURE 37. Difference between $\dot{q}_2$ and $\dot{q}_2^*$ ($k = 20$, initial rectifying ILC).

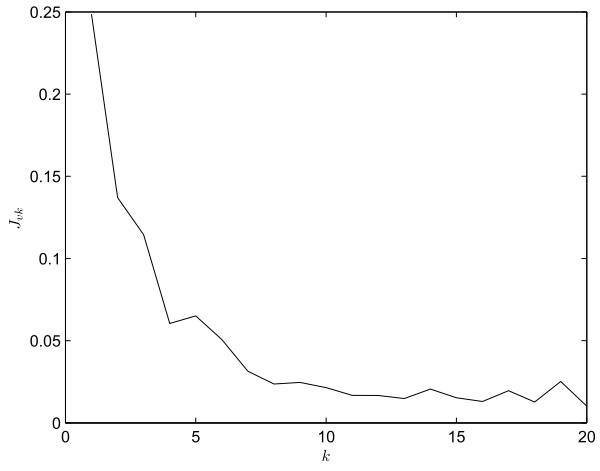

FIGURE 38. Convergence learning history of $\|s_{vk}\|$ (initial rectifying ILC).

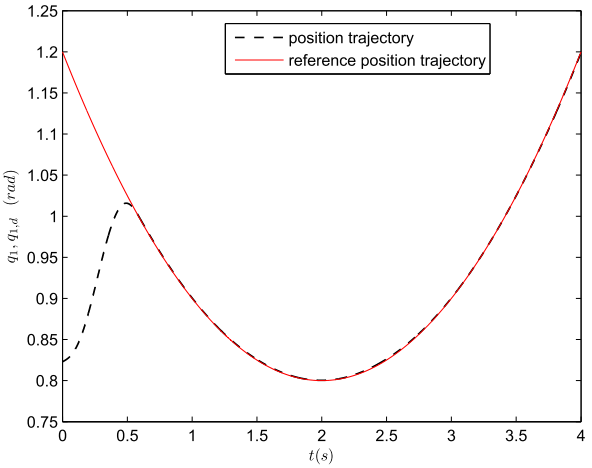

FIGURE 39. Actual and reference position trajectory of joint 1 ($k = 19$, initial rectifying ILC).

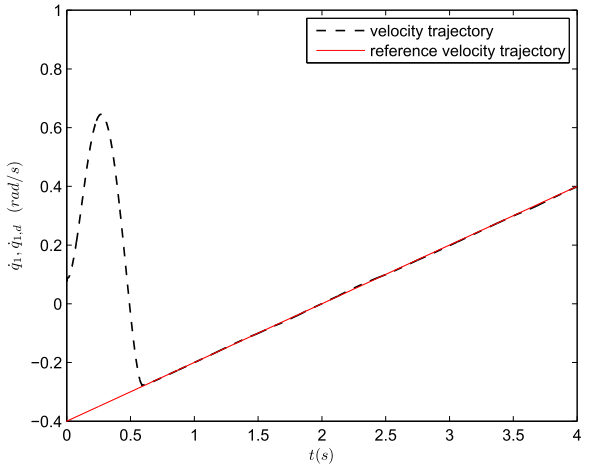

FIGURE 40. Actual and reference velocity trajectory of joint 1 ($k = 19$, initial rectifying ILC).

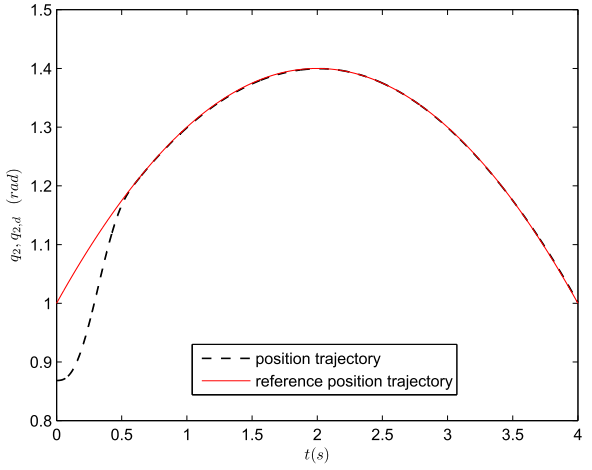

FIGURE 41. Actual and reference position trajectory of joint 2 ($k = 19$, initial rectifying ILC).

cycle, the tracking accuracy of error tracking ILC is a little better than that of initial rectifying ILC. The simulation results verify the effectiveness of our proposed error tracking ILC schme.

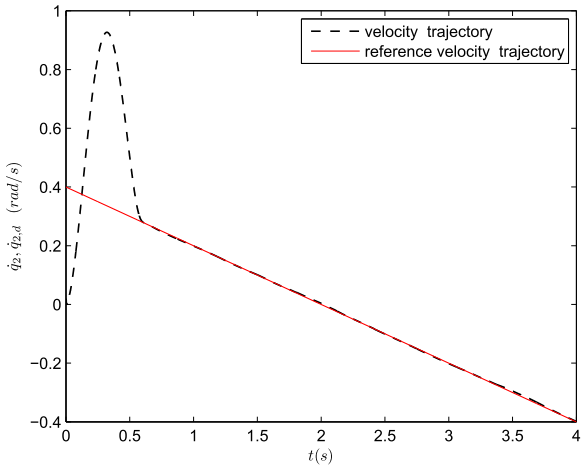

FIGURE 42. Actual and reference velocity trajectory of joint 2 ($k = 19$, initial rectifying ILC).

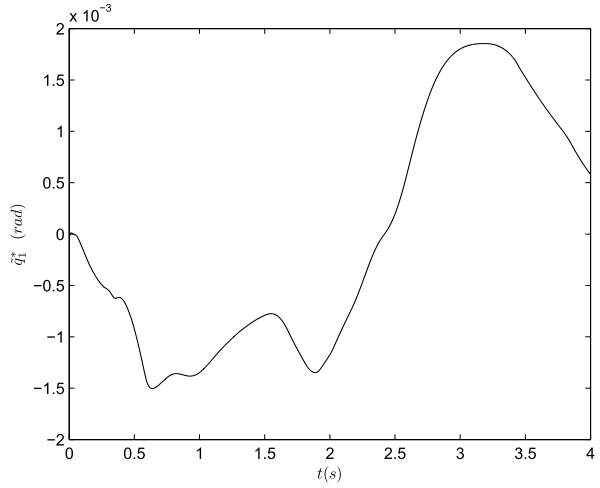

FIGURE 43. Difference between q_1 and q_1^* ($k = 19$, initial rectifying ILC).

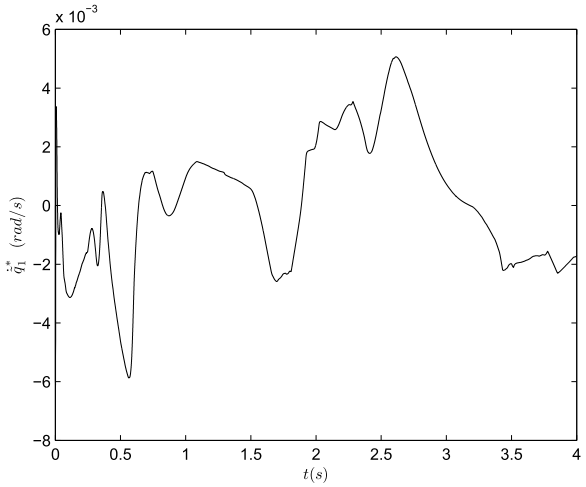

FIGURE 44. Difference between $\dot{q}_2$ and $\dot{q}_2^*$ ($k = 19$, initial rectifying ILC).

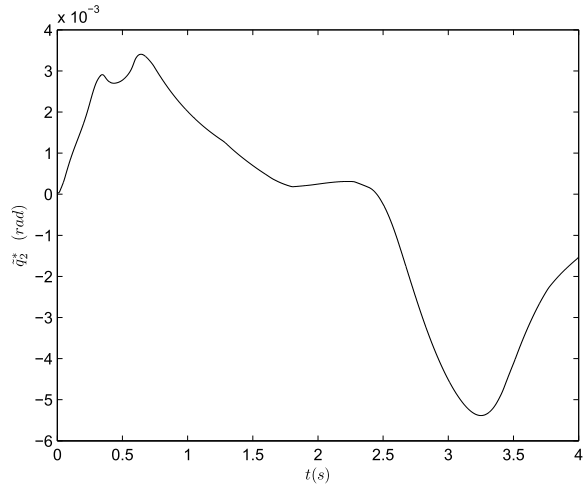

FIGURE 45. Difference between q_2 and q_2^* ($k = 19$, initial rectifying ILC).

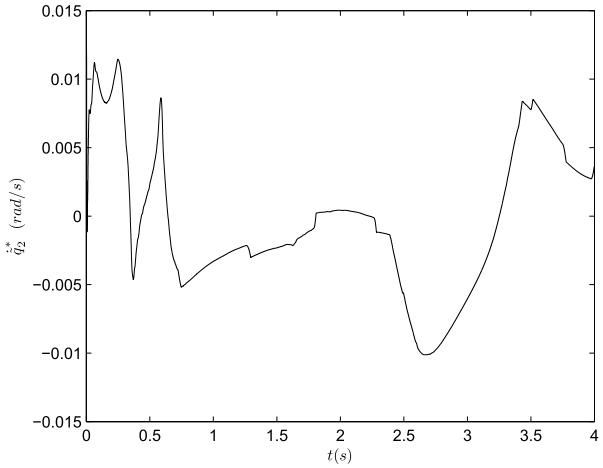

FIGURE 46. Difference between $\dot{q}_2$ and $\dot{q}_2^*$ ($k = 19$, initial rectifying ILC).

It should be noted that the main advantage of error tracking ILC lies in the simplicity of constructing desired error trajectories. As can be seen from equality (5), only $\tilde{q}_{i,k}(0)$ and $\dot{\tilde{q}}_{i,k}(0)$ need to be considered in the construction of $\tilde{q}_{i,k}^*(t)$. During the initial rectifying ILC design for robotic systems, to make rectified reference position trajectory $q_{i,k,r}(t)$ in (49) meet the four requirements, $q_d(t_h)$, $\dot{q}_d(t_h)$ and $\ddot{q}_d(t_h)$ also need to be used in constructing $q_{i,k}^r(t)$, besides $\tilde{q}_{i,k}(0)$ and $\dot{\tilde{q}}_{i,k}(0)$. We need find out $A_{i,5}, A_{i,4}, \cdots, A_{i,0}$ in (51), with the method of undetermined coefficient. By contrast, we can see that constructing desired error trajectories is easier than constructing rectified reference trajectories.

VI. CONCLUSION

In this paper, a robust learning control scheme is proposed to solve the trajectory-tracking problem for robot manipulators with random initial errors and iteration-varying trajectories. Error-tracking strategy is applied to design the controller, with the parametric uncertainties and disturbances compensated by difference learning technique and robust technique, combinedly. A simulation example further verify the theoretical results in the end of this paper. The proposed control

scheme extends the applications of iterative learning control in robotic systems.

REFERENCES

[1] S. Arimoto, S. Kawamura, and F. Miyazaki, "Bettering operation of robots by learning," *J. Robotic Syst.*, vol. 1, no. 2, pp. 123–140, Jun. 1984.
[2] Y. Wang, H. Zhang, S. Wei, D. Zhou, and B. Huang, "Control performance assessment for ILC-controlled batch processes in a 2-D system framework," *IEEE Trans. Syst., Man, Cybern., Syst.*, vol. 48, no. 9, pp. 1493–1504, Sep. 2018.
[3] D. Shen, "Iterative learning control with incomplete information: A survey," *IEEE/CAA J. Autom. Sinica*, vol. 5, no. 5, pp. 885–901, Jul. 2018.
[4] X. Bu, Z. Hou, L. Cui, and J. Yang, "Stability analysis of quantized iterative learning control systems using lifting representation," *Int. J. Adapt. Control Signal Process.*, vol. 31, no. 9, pp. 1327–1336, Sep. 2017.
[5] Y. Li and J. Wei, "Fractional order nonlinear systems with delay in iterative learning control," *Appl. Math. Comput.*, vol. 257, pp. 546–552, Apr. 2015.
[6] Q. Zhu, J.-X. Xu, D. Huang, and G.-D. Hu, "Iterative learning control design for linear discrete-time systems with multiple high-order internal models," *Automatica*, vol. 62, pp. 65–76, Dec. 2015.
[7] T. Hu, K. H. Low, L. Shen, and X. Xu, "Effective phase tracking for bioinspired undulations of robotic fish models: A learning control approach," *IEEE/ASME Trans. Mechatronics*, vol. 19, no. 1, pp. 191–200, Feb. 2014.
[8] X. Dai, S. Tian, Y. Peng, and W. Luo, "Closed-loop P-type iterative learning control of uncertain linear distributed parameter systems," *IEEE/CAA J. Automatica Sinica*, vol. 1, no. 3, pp. 267–273, Jul. 2014.
[9] P. Bondi, G. Casalino, and L. Gambardella, "On the iterative learning control theory for robotic manipulators," *IEEE J. Robot. Autom.*, vol. 4, no. 1, pp. 14–22, Feb. 1998.
[10] J.-X. Xu and Y. Tan, "A composite energy function-based learning control approach for nonlinear systems with time-varying parametric uncertainties," *IEEE Trans. Autom. Control*, vol. 47, no. 11, pp. 1940–1945, Nov. 2002.
[11] A. Tayebi, "Adaptive iterative learning control for robot manipulators," *Automatica*, vol. 40, no. 7, pp. 1195–1203, Jul. 2004.
[12] C.-J. Chien and A. Tayebi, "Further results on adaptive iterative learning control of robot manipulators," *Automatica*, vol. 44, no. 3, pp. 830–837, Mar. 2008.
[13] F. Cao and J. Liu, "An adaptive iterative learning algorithm for boundary control of a coupled ODE–PDE two-link rigid–flexible manipulator," *J. Franklin Inst.*, vol. 354, no. 1, pp. 277–297, Jan. 2017.
[14] X. Li, Y.-H. Liu, and H. Yu, "Iterative learning impedance control for rehabilitation robots driven by series elastic actuators," *Automatica*, vol. 90, pp. 1–7, Apr. 2018.
[15] X.-D. Li, M.-M. Lv, and J. K. L. Ho, "Adaptive ILC algorithms of nonlinear continuous systems with non-parametric uncertainties for non-repetitive trajectory tracking," *Int. J. Syst. Sci.*, vol. 47, no. 10, pp. 2279–2289, 2016.
[16] X. Ruan and Z. Z. Bien, "Pulse compensation for PD-type iterative learning control against initial state shift," *Int. J. Syst. Sci.*, vol. 43, no. 11, pp. 2172–2184, Nov. 2012.
[17] D. Meng, Y. Jia, J. Du, and F. Yu, "Robust design of a class of time-delay iterative learning control systems with initial shifts," *IEEE Trans. Circuits Syst. I, Reg. Papers*, vol. 56, no. 8, pp. 1744–1757, Aug. 2009.
[18] Q. Z. Yan and M. X. Sun, "Error-tracking iterative learning control with state constrained for nonparametric uncertain systems," *Control Theory Appl.*, vol. 32, no. 7, pp. 895–901, Jul. 2015.
[19] Q. Z. Yan and M. X. Sun, "Iterative learning control for nonlinear uncertain systems with arbitrary initial state," *Acta Autom. Sinica*, vol. 42, no. 4, pp. 545–555, Apr. 2016.
[20] Q. Z. Yan, M. X. Sun, and H. Li, "Consensus-error-tracking learning control for non parametric uncertain multi-agent systems," *Control Theory Appl.*, vol. 33, no. 6, pp. 793–799, Jun. 2016.
[21] X. Zhu and J. Wang, "Double iterative compensation learning control for active training of upper limb rehabilitation robot," *Int. J. Control, Autom. Syst.*, vol. 16, no. 3, pp. 1312–1322, Jun. 2018.
[22] M.-X. Sun, X.-X. He, and B.-Y. Chen, "Repetitive learning control for time-varying robotic systems: A hybrid learning scheme," *Acta Automatica Sinica*, vol. 33, no. 11, pp. 1189–1195, Nov. 2007.
[23] X. Jin and J.-X. Xu, "A barrier composite energy function approach for robot manipulators under alignment condition with position constraints," *Int. J. Robust Nonlinear Control*, vol. 24, no. 17, pp. 2840–2851, 2014.
[24] S. S. Saab, W. G. Vogt, and M. H. Mickle, "Learning control algorithms for tracking 'slowly' varying trajectories," *IEEE Trans. Syst., Man, Cybern., B (Cybern.)*, vol. 27, no. 4, pp. 657–670, Aug. 1997.
[25] J.-X. Xu and J. Xu, "On iterative learning from different tracking tasks in the presence of time-varying uncertainties," *IEEE Trans. Syst., Man, Cybern., B (Cybern.)*, vol. 34, no. 1, pp. 589–597, Feb. 2004.
[26] J.-M. Li, Y.-P. Sun, and Y. Liu, "Hybrid adaptive iterative learning control of non-uniform trajectory tracking," *Control Theory Appl.*, vol. 25, no. 1, pp. 100–104, Jan. 2008.
[27] C. J. Chien, "A combined adaptive law for fuzzy iterative learning control of nonlinear systems with varying control tasks," *IEEE Trans. Fuzzy Syst.*, vol. 16, no. 1, pp. 40–51, Feb. 2008.
[28] R. Chi, Z. Hou, and J.-X. Xu, "Adaptive ILC for a class of discrete-time systems with iteration-varying trajectory and random initial condition," *Automatica*, vol. 44, no. 8, pp. 2207–2213, Aug. 2008.
[29] X.-D. Li, T. W. S. Chow, and L. L. Cheng, "Adaptive iterative learning control of non-linear MIMO continuous systems with iteration-varying initial error and reference trajectory," *Int. J. Syst. Sci.*, vol. 44, no. 4, pp. 786–794, 2013.
[30] J.-J. E. Slotine and L. Weiping, "Adaptive manipulator control: A case study," *IEEE Trans. Autom. Control*, vol. AC-33, no. 11, pp. 995–1003, Nov. 1988.
[31] C.-Y. Su and T. P. Leung, "A sliding mode controller with bound estimation for robot manipulators," *IEEE Trans. Robot. Autom.*, vol. 9, no. 2, pp. 208–214, Apr. 1993.
[32] J.-J. E. Slotine and W. Li, *Applied Nonlinear Control*. Englewood Cliffs, NJ, USA: Prentice-Hall, 1991.
[33] J.-X. Xu and R. Yan, "On initial conditions in iterative learning control," *IEEE Trans. Autom. Control*, vol. 50, no. 9, pp. 1349–1354, Sep. 2005.
[34] M. Sun, T. Wu, L. Chen, and G. Zhang, "Neural AILC for error tracking against arbitrary initial shifts," *IEEE Trans. Neural Netw. Learn. Syst.*, vol. 29, no. 7, pp. 2705–2716, Jul. 2018.

QIUZHEN YAN received the M.S. degree in computer science and the Ph.D. degree in control science and engineering from the Zhejiang University of Technology, Hangzhou, China, in 2005 and in 2015, respectively. Since 2005, he has been with the College of Information Engineering, Zhejiang University of Water Resources and Electric Power, where he is currently a Lecturer. His current research interests include iterative learning control and repetitive control. He is a member of the Chinese Association of Automation.

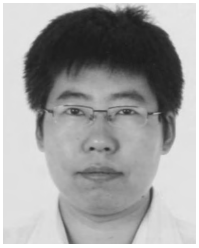

JIANPING CAI received the Ph.D. degree from Zhejiang University, in 2014. He is currently a Professor with the School of Electronical Engineering, Zhejiang University of Water Resources and Electric Power. His current research interests include nonlinear systems and adaptive control.

YAN MA received the B.S. degree in industrial automation from the China University of Mining and Technology, in 2001, and the M.S. degree in control theory and control engineering from the Zhejiang University of Technology. In 2004, she came to the Zhejiang University of Water Resources and Electric Power and became an Assistant with the Information Engineering and Art Design Department, Hangzhou, where she has been a Lecturer, since 2004. Her current research interests include automatic control and industrial automation.

YOUFANG YU received the B.S. degree in electronic engineering and the M.S. degree in agricultural electrification and automation from Zhejiang University, Hangzhou, in 1999 and in 2006, respectively. From 1999 to 2003, she was a Lecturer with the Anhui Vocational and Technical College, Hefei. From 2006 to 2008, she became an Electronic Engineer with the Research and Development Department, Zhejiang Jincheng Technology Development Co., Ltd., Hangzhou. Since 2008, she has been with the Applied Engineering College, Zhejiang Business College, Hangzhou. She is currently an Associate Professor. Her current research interests include automatic control, industrial automation, electronic technology, and biomass technology.